Optical Engineering

OpticalEngineering.SPIEDigitalLibrary.org

Comparative study of light propagation and single-mode operation in large-mode area fibers designed for 2-μm laser applications

Clémence Jollivet
Bryce Samson
Lasse Leick
Lawrence Shah
Martin Richardson
Axel Schülzgen

SPIE.

Comparative study of light propagation and single-mode operation in large-mode area fibers designed for 2-μm laser applications

Clémence Jollivet,[a,*] Bryce Samson,[b] Lasse Leick,[c] Lawrence Shah,[a] Martin Richardson,[a] and Axel Schülzgen[a]
[a]CREOL, College of Optics and Photonics, University of Central Florida, Orlando, Florida 32816, United States
[b]Nufern, East Granby, 7 Airport Park Road, Connecticut 06026, United States
[c]NKT Photonics, Blokken 84, Birkerød 3460, Denmark

Abstract. Output performances of fiber-based optical systems, in particular fiber lasers and amplifiers, can be controlled using tailored fiber designs, gain profiles, and pump light overlap with the gain medium. Here, the performances of 2-μm light, propagating in three large-mode area fibers, a step-index fiber, a photonic crystal fiber (PCF), and a leakage channel fiber (LCF), designed to deliver a single-mode (SM) beam at this wavelength, were compared. Using the S^2 imaging technique, the transverse mode content has been decomposed, and propagation losses, SM purity, and mode-field area (MFA) were measured for various input mode overlap and coiling diameters. It was experimentally demonstrated that coiling the PCF and LCF to 40 and 20 cm in diameter, respectively, resulted in efficient higher-order mode suppression, pure SM beam delivery, moderate (~1 dB) coil-induced losses in the fundamental mode, and nondistorted, large MFA (~1600 μm^2) beam delivery.
 [DOI: 10.1117/1.OE.54.1.011006]

Keywords: fiber lasers; large-mode area fiber; specialty fiber design; fiber characterization; mode analysis.

Paper 140704SS received Apr. 30, 2014; revised manuscript received Jul. 28, 2014; accepted for publication Aug. 6, 2014; published online Aug. 25, 2014.

1 Introduction

The scientific interest in developing light sources emitting around the wavelength of 2 μm has been motivated by the discovery of novel light-matter interaction and light propagation phenomena, as well as the wide range of existing and potential future applications using light at this eye-safe wavelength. To date, a number of successful applications were reported including directed energy and long range atmospheric propagation, spectroscopy, LIDAR, medical surgery as well as pumping of mid-IR light sources.[1–5] Taking on the advantages offered by the fiber technology in terms of low attenuation, high doping concentrations, compactness, stability, efficiency, and competitive cost, a significant number of studies have been focused, during the past few years, on developing novel 2-μm laser and amplifier sources using Thulium (Tm)-doped optical fibers.[6]

During the past few years, scaling the fiber laser performances to achieve high power, high efficiency, and excellent beam quality has been an on-going research topic which strongly depended on the development of novel fiber designs. In this context, a critical design consideration to control the beam quality and the laser emission performances has been to limit the number of guided higher-order modes (HOMs), while increasing the area of the fundamental mode (FM), in order to increase the damage threshold of fused silica and decrease the onset of nonlinear effects. For this purpose, specialty fiber designs, called large-mode area (LMA) fibers, have been fabricated and successfully implemented in fiber lasers using step-index fibers (SIFs),[7] photonic crystal fibers (PCFs),[8,9] and large-pitch fibers.[10] However, it is worth noting that, even though the HOM content is strongly attenuated in LMA fiber designs, a residual amount of HOM is often weakly guided in the core, which might induce beam distortions, beam walking, and pointing instabilities as well as degradation of the pulse energy in Q-switched Tm-doped fiber lasers.[11] Furthermore, thermal modal instabilities, triggered by seemingly negligible HOM contents and resulting in severe beam degradation above a specific laser power threshold, have been reported in LMA fiber lasers and are, currently, the bottle-neck for further power scaling.[12,13]

Among the different techniques available to quantify and avoid beam degradations, the measurement of the spatial beam quality factor, the so-called M^2 parameter, is by far the most common one with $M^2 = 1$ corresponding to an ideal Gaussian beam.[14,15] However, it has also been demonstrated that the beams exhibiting Gaussian-like profiles could contain small fractions of HOMs.[16] Accurately evaluating the residual HOM content required in-depth experimental diagnostic techniques able to decompose the guided light into individual transverse modes. In particular, the spatially and spectrally resolved imaging, also called S^2 imaging, introduced in Sec. 3, has been widely employed to measure residual HOM content in LMA fibers, attenuated as low as ~ -40 dB, with an unmatched accuracy. Thus, using S^2 imaging appeared to be a suitable approach to validate the ability of novel fibers, initially designed to operate in the pure single-mode (SM) regime, to achieve such performances and to contribute to improving laser performances.

In the present work, three different LMA fibers, an SIF, a PCF, and a leakage channel fiber (LCF), designed for 2-μm applications were used and are presented in detail in Sec. 2. Then, in Sec. 3, the transverse mode content propagating at

*Address all correspondence to: Clémence Jollivet, E-mail: jollivet@creol.ucf.edu

0091-3286/2015/$25.00 © 2015 SPIE

a 2-μm light wavelength in each fiber was decomposed using S^2 imaging mode analysis for various input mode overlap and as a function of coiling diameters. The measured modal properties were directly compared between the LMA fibers in order to experimentally determine the impact of the fiber design on the properties of the propagating light. Finally, in Sec. 4, the respective ability of the SIF, PCF, and LCF to deliver ultrapure SM beams with a large mode-field area (MFA) is discussed.

2 LMA Fiber Designs: Structures and Modal Properties

The selected LMA fiber cores were passive structures, primarily designed for power scaling applications of laser and amplifier systems emitting diffraction limited beam quality at wavelengths around 2 μm. A microscope image of each LMA fiber sample is shown in Fig. 1. In Fig. 1(a), a polarization maintaining (PM) SIF design with a 25-μm-diameter core, 400-μm-diameter cladding, and ~0.08 numerical aperture (NA) was used. This fiber has been fabricated by Nufern (East Granby, Connecticut), and similar designs using a Tm-doped core have been implemented in 2-μm high-power monolithic fiber lasers.[8,17] The LMA SIF design was directly compared with a PM PCF, made by NKT Photonics (Birkerød, Denmark), with a 50-μm-diameter core, ~0.06 NA, surrounded by a periodic array of air-holes and a pump cladding of 250 μm in diameter. Several studies have been reported using Tm-doped versions of this LMA PCF design in continuous wave and Q-switched laser cavities.[9,18] The third design was an LCF prototype specialty design conceived by Nufern with a 50-μm-core diameter, ~0.07 NA and surrounded by two layers of fluorine-doped rods embedded in a fused-silica matrix forming the cladding. The LCF is an all-solid design offering a promising alternative for the power scaling of fiber lasers.[19] Even though the selected LCF has not been specifically designed for 2-μm applications, low propagation losses were recently reported at this wavelength.[20] A summary of the manufacturer-specified dimensions can be found in Table 1.

In order to predict and compare the number of mode supported in each fiber at the light wavelength of 2 μm, a finite element mode solver has been used (Fimmwave, by PhotonDesign, Oxford, United Kingdom). To ensure accurate results, the fiber dimensions were measured using the microscope images shown in Fig. 1, and the refractive indices for each LMA fiber layer have been measured with a profilometer (by Interfiber Analysis, Sharon, Massachusetts). For completeness, the mode-field diameter (MFD) of the FM has been calculated and results are summarized in Table 1. Mode solver calculations were performed at the wavelength of interest and results are plotted in Fig. 1(d), showing the effective Δn, the effective difference between modes and cladding indices, of the first linearly polarized (LP) modes that are guided in each LMA fibers. A positive Δn value indicates a core mode, whereas a negative Δn corresponds to a cladding mode. As a result, five modes (LP_{01}, LP_{11}, LP_{21}, LP_{02}, and LP_{31}) can be supported in the core of the SIF while only LP_{01} and LP_{11} can be expected to be guided in the core of the PCF and LCF.

Table 1 Selected large-mode area (LMA) fiber design specifications.

	Step-index fiber (SIF) LMA	Photonic crystal fiber (PCF) LMA	Leakage channel fiber (LCF) LMA
Core/cladding diameter (μm)	25/400	50/250/550	50/440
Core numerical aperture	0.08	0.06	0.07
Mode-field diameter (calculated at 2 μm)	24	35	42
Fiber length (m)	3.1	2.3	9.0

3 Mode Analysis of the LMA Fibers at 2 μm

To decompose transverse modes guided in each LMA fibers [Figs. 1(a)–1(c)], the S^2 imaging mode analysis technique, demonstrated by Nicholson et al.,[21] has been performed. A schematic of the experiment is presented in Fig. 2. This technique has gained significant interest during the past few years for its ability to resolve the amplitude and phase profile of weakly guided modes, particularly in specialty

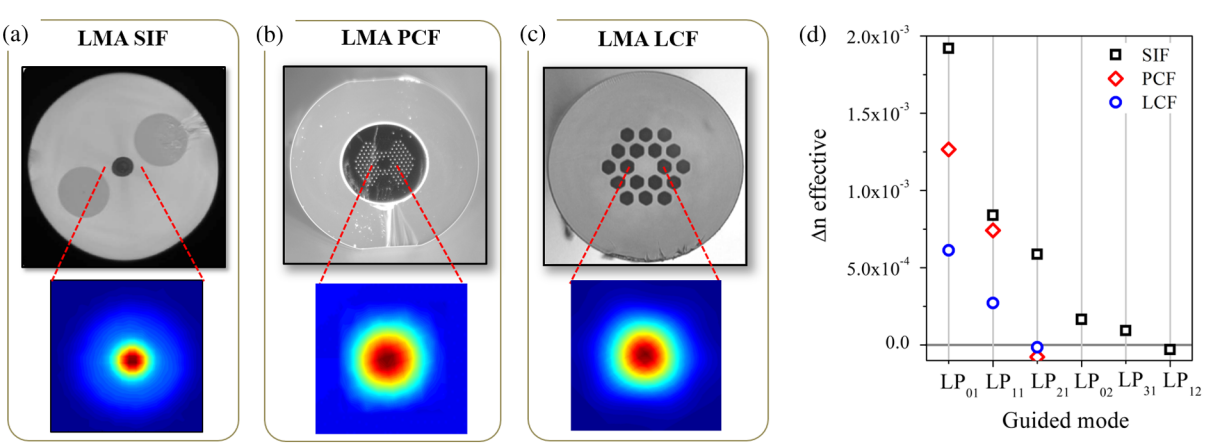

Fig. 1 Microscope images of the facets of the large-mode area (LMA) step-index fiber (SIF) (a) photonic crystal fiber (PCF) (b) and leakage channel fiber (LCF) (c) with charge-coupled device (CCD) recorded beam profiles emerging from the fiber core after propagation of 2-μm light. (d) Effective Δn values calculated for the first LP modes in the selected LMA fibers at this wavelength.

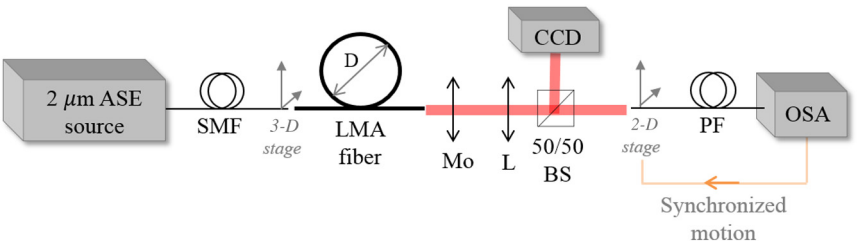

Fig. 2 Schematic of S^2 imaging technique for decomposing individual transverse modes guided in a LMA fiber. Mo: microscope objective; L: lens; BS: beam splitter; PF: probe fiber.

fibers. Using a broadband Tm-doped fiber-coupled amplified spontaneous emission source emitting light from 1.92 to 1.96 μm wavelength, the modes in the LMA fiber under test were excited. The input single-mode fiber (SMF), used to deliver the light, was mounted on a 3-axis stage and butt-coupled to the LMA fiber under investigation.

Since S^2 imaging is a measurement of the multimode interference (MMI) which depends on the modal properties in each fiber design, the length of each LMA fiber has been carefully chosen to ensure a high spectral resolution (~30 MMI periods) within the measurement bandwidth ($\Delta\lambda =$ 40 nm). Fiber length values can be found in Table 1. Using the axis of the three-dimensional (3-D) stage, mode-field matching was adjusted between the delivery SMF and the LMA fiber to minimize coupling losses and optimize mode overlap between the SMF Gaussian beam and the FM of the LMA fiber. During this preliminary alignment procedure, the near-field of the beam emerging the LMA fiber was monitored with a charge-coupled device (CCD). Measured profiles emerging the SIF, the PCF, and the LCF designs are shown in Figs. 1(a), 1(b), and 1(c), respectively, showing a smooth, Gaussian-like spatial distribution.

The modal decomposition of the fiber under test required several steps: was obtained after (a) imaging the LMA fiber near-field on the tip of a probe fiber (PF) using a 50/50 beam splitter, (b) recording the MMI spectra using an optical spectrum analyzer (OSA, Yokogawa with a 1.2 to 2.4-μm wavelength range, Yamanashi, Japan), and (c) repeating the MMI measurement while scanning the PF across the LMA fiber near-field. The data acquisition was synchronized between the PF motion and the OSA recording time to ensure an efficient measurement procedure. Individual mode amplitude and phase profiles, as well as the fraction of power carried by each mode, either called mode power ρ^2 (normalized) or multipath interference (MPI, in dB), were measured using an appropriate Fourier treatment of the recorded spectra.[21,22] Several evaluation algorithms, based on different assumptions on the guided mode content, have been proposed to evaluate ρ^2 and MPI.[23] It has been demonstrated that the result's accuracy depends on the choice of the mode power evaluation algorithm.[24] In the present study, method 2 of Otto et al.[23] was employed to evaluate ρ_n^2 for the n'th guided mode and the MPI was directly calculated as $10 \times \log(\rho_n^2)$. This approach has been demonstrated to provide the highest accuracy when evaluating modes carrying up to 30% of the total power.[24]

3.1 *Effect of In-Coupling Alignment on Modal Content*

Due to the significant dimension mismatch between the LMA fibers and the conventional fiber components, most LMA-based fiber lasers are assembled in cavity architectures using free-space sections. In such cases, imaging schemes are designed using specific lens combinations to optimize the coupling efficiency in the core of the LMA fibers. In addition, it is well known from the general waveguide theory that the mode combination excited in an optical fiber depends on the overlap between the incident field and the allowed guided modes. For example, for a centered alignment between the core of the SMF and the LMA, the power will be only coupled in circularly symmetric modes labeled $LP_{0,n}$.

In order to evaluate the response of LMA fiber designs to change the input mode overlap, S^2 imaging was performed on the three LMA fibers for two coupling alignments, centered and off-centered, while maintaining the fibers unperturbed (coil diameter >60 cm to avoid any influence of the fiber bend on the guided mode content). The measurement is initiated by finding the centered alignment position. To do so, the in-coupling SMF position is adjusted using the 3-D stage with respect to the LMA fiber core while imaging the fiber near-field on the CCD. Once the imaged beam exhibits a uniform Gaussian-like profile, the stage is translated by 2 μm to create an intentional in-coupling offset. Results of S^2 imaging performed on the LMA SIF are presented in Fig. 3(a), where the calculated Fourier spectra corresponding to the centered and 2-μm off-centered mode analysis were plotted in plain and dashed lines, respectively. The corresponding near-field profiles measured with the CCD are shown in the inset of Fig. 3(a) (top and bottom respectively). In the Fourier domain, the differential group delays (DGDs) of the various guided modes interfering, respectively, with the FM are indicated using arrows. For centered in-coupling alignment, about 73% of the power was measured to be in the FM while up to 20% was carried in the HOM LP_{02} (corresponding MPI $= -7$ dB) and a few percent in LP_{11} (MPI $=$ -21 dB). In comparison, four HOMs could be resolved after creating a 2-μm offset of the in-coupling alignment. From the S^2 imaging analysis, the guided mode amplitude ($E_{0,n}$) and phase (φ_n) profiles have been reconstructed and results are presented in Figs. 3(b)–3(e) and 3(f)–3(i), respectively. The HOMs LP_{11}, LP_{21}, LP_{02}, and LP_{31} can be identified indicating a total of five modes including the FM propagating in the LMA SIF. These results are in very good agreement with the mode solver results shown in Fig. 1(d). The mode power distribution has been calculated and the MPI results are plotted in Fig. 3(j) for the center (full markers) and off-center (empty markers) alignments. These measurements confirm that a small in-coupling offset alignment in the LMA fiber directly influences the modal combination, increasing the amount of HOM guided in the

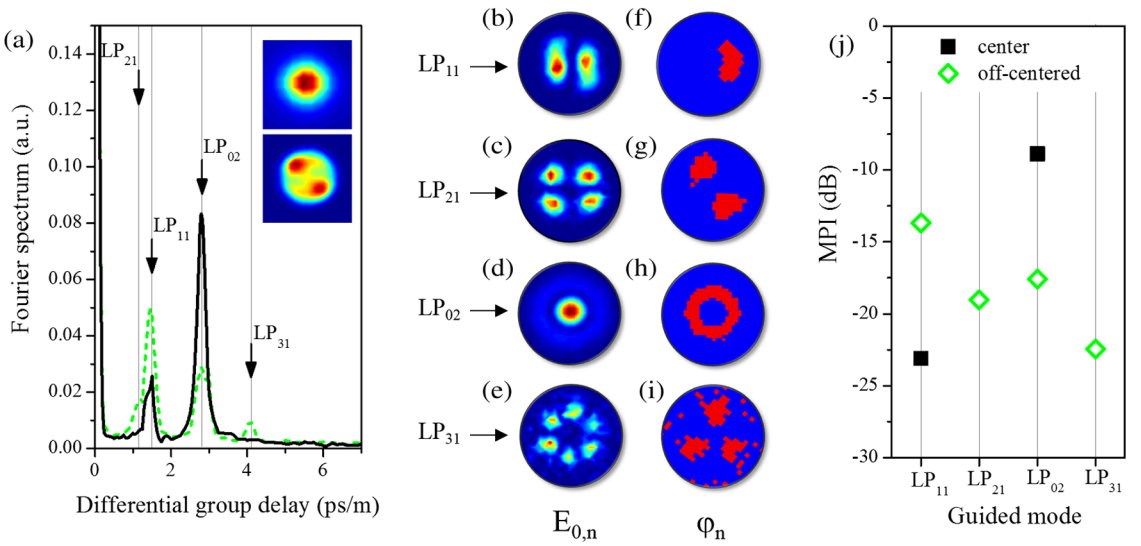

Fig. 3 (a) S^2 imaging Fourier spectra of the LMA SIF measured at 2 μm for two different in-coupling alignments: centered (plain line) and 2-μm lateral offset (dashed line). The intensity of the corresponding beams emerging the SIF, measured on a CCD, is shown in inset. The decomposed guided higher-order mode (HOM) content is indicated with arrows. From (b) to (e), the modal amplitude $E_{0,n}$ and from (f) to (i) phase φ_n have been reconstructed for the measured LP_{11}, LP_{21}, LP_{02}, and LP_{31} guided HOMs. The multipath interference (MPI) values are plotted in (j) for centered and offset excitation in full and empty markers, respectively.

fiber. As a result, lasing performances in terms of stability, efficiency, and beam profile can be directly impacted.

The influence of the in-coupling alignment on the mode content has also been measured, using S^2 imaging, in the LMA PCF and the LCF. According to the mode analysis results, the HOM LP_{11} was guided in both fiber designs around a 2-μm light wavelength regardless of the coupling alignment. Measured MPI values are summarized in Table 2 showing that, even for optimum coupling (0-μm lateral offset) corresponding to uniform near-field profiles in Figs. 1(b) and 1(c) measured with the CCD, a residual amount of HOM LP_{11}, 1.4% of the light guided in the PCF (−18.4 dB), and 4.7% in the LCF (−13.2 dB) could be measured with S^2 imaging. This fraction of HOM can be attributed to experimental imperfections in the fiber coupling alignment and to a small mode mismatch between the input Gaussian beam and the LMA fiber FM. As the SMF to the LMA fiber mode matching was intentionally perturbed (introduction of a 2-μm lateral offset), no additional HOM rather than LP_{11} could be measured, which is in agreement with the numerical predictions in Fig. 1(d). However, as expected with the introduction of an in-coupling mode mismatch, the fraction of light carried by the LP_{11} mode increased in both LMA fibers by ∼2 dB.

It is important to detect and quantify residual amount of HOMs, in particular when employing LMA fibers in laser cavities toward power scaling applications where the residual power carried by the HOMs could, under amplification, cause deterioration of the laser performances above certain power levels.

Table 2 Multipath interference values (in dB) of LP_{11} content measured by S^2 imaging analyses.

Lateral offset (μm)	PCF LMA	LCF LMA
0	−18.4	−13.2
2	−16.1	−11.7

3.2 *Coiling-Induced HOM Suppression*

In order to suppress the residual HOM content guided in the LMA fiber designs previously measured in Sec. 3.1, a widely employed technique is to coil the fiber in order to convert core modes into cladding modes.[25,26] Here, S^2 imaging was performed while changing the coiling diameter for a fixed coupling alignment corresponding to the optimized launching. In order to directly compare the coil-induced HOM suppression between the different fiber designs, the total length of the coiled fiber (∼1.9 m) remained constant for the three LMA fibers by adjusting the number of coiled loops. The rest of the fiber length was stabilized with a diameter larger than 60 cm to avoid unwanted influence on the HOM content. The Fourier spectra calculated for the LMA SIF, the PCF, and the LCF are presented in Figs. 4(a), 4(b), and 4(c), respectively. The corresponding mode powers have been evaluated and the results are plotted in Fig. 5. In Fig. 4(a), the HOM LP_{02}, which carried a significant amount of light in the straight LMA SIF under optimized coupling, is strongly attenuated due to bend-induced losses, down to 17-dB attenuation for coil diameter of 10 cm. In the meantime, instead of experiencing coil-induced losses, the measured LP_{11} MPI slightly increased (square markers in Fig. 5). A possible reason for this effect can be that, as the fiber birefringence considerably increased due to the tight coiling diameter, the LP_{02} mode power not only transferred to cladding modes but also to guided HOMs such as LP_{11} and LP_{21} modes. The measured residual LP_{21} excited at $D = 10$ cm was measured at DGD = 1.1 ps/m [dashed curve in Fig. 4(a)] and intentionally not represented for

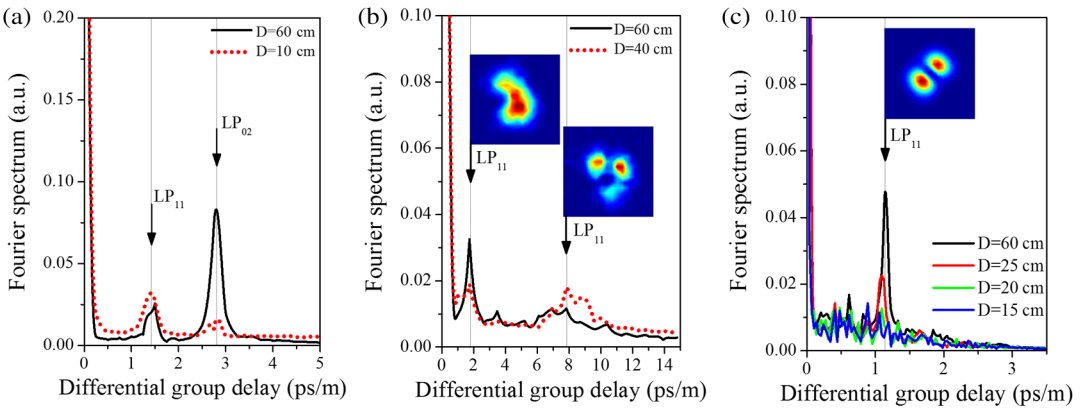

Fig. 4 S^2 imaging Fourier spectra of the LMA SIF (A), PCF (b), and LMA LCF (c) for various coiling diameters. The guided HOMs are indicated with an arrow and the corresponding reconstructed modal amplitude is shown in the respective inset.

clarity reasons. In the LMA PCF, on the other hand, it was found that efficient HOM suppression could be achieved using coiling diameters of 40 cm as the initially guided HOM LP_{11} experienced significant losses in Fig. 4(b). As LP_{11} is suppressed, however, the DGD difference broadens and shifts toward higher values while a small amount of power was still carried by the HOM. This was confirmed after reconstructing the amplitude profile has been reconstructed in Fig. 4(b) at the two DGD values, where beam distortion toward LP_{11} could be measured. Finally, coil-induced HOM suppression in the LCF has been measured and the results are presented in Fig. 4(c). As shown on the Fourier spectra, the initially guided LP_{11} mode measured around DGD $= 1.2$ ps/m could be efficiently suppressed when coiling the fiber down to 20 and 15 cm in diameter.

The mode power evaluation corresponding to the S^2 imaging mode analyses measurements shown in Fig. 4 is summarized in Fig. 5, where the MPI of the guided HOM has been calculated and was plotted as a function of the coiling diameter for the three LMA fiber designs under investigation: SIF with square, PCF with diamond and LCF with circle shaped markers. Open markers correspond to LP_{11} MPI values while filled markers denote LP_{02}. According to Fig. 5, the MPI of LP_{11}, the only HOM guided in LMA PCF and LCF designs, could be reduced by ~5 and ~18 dB after coiling the fibers around 40 and 15-cm diameters, respectively. The remaining amount of LP_{11} corresponds to $\rho^2 = 0.5\%$ and 0.07% in the LMA PCF and LCF designs, respectively. In the SIF, however, while LP_{02} is efficiently suppressed (MPI reduced by ~20 dB), the LP_{11} mode could not be efficiently suppressed with ~2.5% of light remaining.

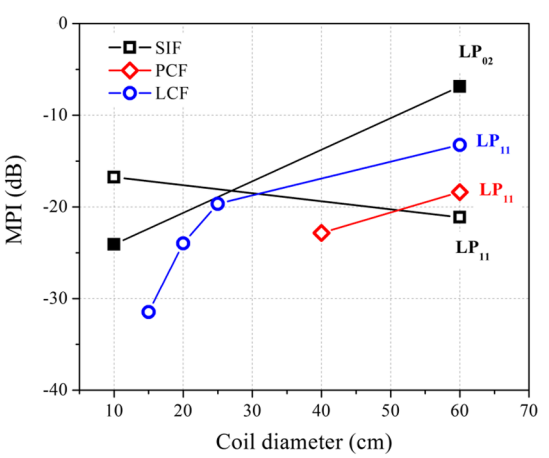

Fig. 5 Measured MPI in the SIF, PCF, and LCF designs represented using square, diamond, and circle markers for various coiling diameters. The MPI of LP_{11} was represented using open markers while filled markers correspond to LP_{02} (only measured in the SIF). Lines are shown for guidance of the eye.

4 Discussion: Comparison between SM Performances of Different LMA Fiber Designs

4.1 *SM Purity*

In this section, the SM purity, defined as the fraction of power carried by the FM during light propagation, was measured using the S^2 imaging analysis results. From the mode power values, the SM purity was calculated by subtracting the sum of the measured HOM content from the total value of 1. Results are plotted in Fig. 6 as a function of coil diameter for the LMA SIF, the PCF, and the LCF with square, diamond, and circle-shaped markers, respectively. According to S^2 imaging mode analyses results detailed in Sec. 3.2, it was demonstrated that ~100% SM purity was achieved in the PCF and the LCF designs at a critical SM coiling diameter, labeled D_{SM}, equal to $D_{SM} = 40$ and 20 cm, respectively. These values are indicated with filled markers in Fig. 6, respectively. In contrast, only a 90% SM purity could be achieved in the SIF design indicating that, even after coiling the fiber around a tight loop of 10 cm in diameter, a fraction of the light was still carried by HOM, mainly by LP_{11}. Tighter coiling of this fiber was limited by the relatively thick outer diameter of 400 μm and pure SM propagation could not be reached.

For completeness, in the PCF and the LCF where SM operation could be achieved, the coil-induced losses experienced by the FM were evaluated and compared between the two designs in order to characterize the best fiber design performances in terms of core confinement. To do so, the total amount of power transmitted by the fiber core was measured for each coiling measurement shown in Fig. 6. From the knowledge of the fraction of light carried by the HOM (using S^2 imaging results of Figs. 4 and 5), the percentage

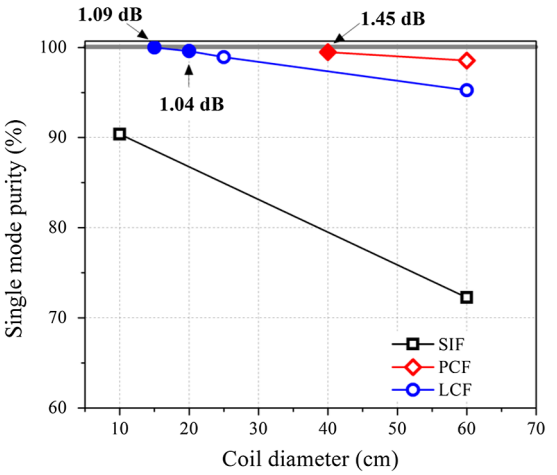

Fig. 6 Single-mode (SM) purity of the 2-μm beam emerging from the SIF (square), PCF (diamond), and LCF (circle) as function of coiling diameter. SM regimes are indicated by plain markers. The values indicate the overall bend-induced losses measured at specific coil diameters.

of light carried by the FM could be extracted for each coiling diameter and the corresponding coil-induced attenuation was measured. Numbers are indicated in Fig. 6 with arrows for different coiling diameters. The FM guided in the PCF experiences higher bend-induced losses, i.e., lower core confinement, than the FM guided in the LCF core. Furthermore, it was possible to reach an ultrapure SM regime in the LCF where more than 99.9% of the light was measured in the FM for $D_{SM} = 15$ cm while maintaining a very good core confinement. As a result, it was possible to reach a pure SM regime in both LMA PCF and LCF designs during propagation of a 2-μm light wavelength, offering a strong potential for high performance fiber laser applications.

4.2 *Mode Effective Area and Beam Distortions*

In this section, the effect of bend-induced HOM suppression on the MFA and the spatial uniformity of the emerging beam has been investigated using the S^2 imaging mode decomposition results. In addition, tight coiling of LMA fibers also influences the profiles of the emerging beam.[26] To measure and compare the measured MFA between the LMA fiber designs, the near-field of the total beam emerging the fibers has been measured using a CCD (1) after a 2-μm wavelength light propagation in straight fibers [Figs. 1(a)–1(c)] and (2) after coiling each fiber at the SM diameter, labeled D_{SM}, determined from S^2 imaging analysis and summarized in Fig. 6. The beam emerging fibers coiled at D_{SM} (or smallest coil diameter in the case of the SIF) have been recorded and are shown in Figs. 7(a)–7(c), after the SIF, PCF, and LCF, respectively. Whereas the SIF profile exhibits strong spatial distortions corresponding to the residual amount of LP_{11} and LP_{21} (measured in Figs. 4(a) and 5), both PCF and LCF deliver a SM beam with good spatial uniformity.

The MFA of the beam delivered by the PCF and the LCF were measured by applying a Gaussian-fitting function to the recorded beam profiles for $D > 60$ cm [Figs. 1(b) and 1(c), representing the case of an unperturbed and straight fiber] and at D_{SM} (determined in Fig. 6 after S^2 imaging analysis). The MFA values were calculated after extraction of the MFD, defined at $1/e^2$ from the intensity maximum. Results for both fibers are plotted in Fig. 7(d). Filled symbols denote pure SM light propagation at D_{SM} corresponding to 40 cm for the PCF and 15 cm for the LCF. The coefficient of determination of the Gaussian fit, labeled R^2, is shown in Fig. 7(d) indicating a very good fit quality. The MFA of the beam emerging from the PCF and the LCF designs experience a decrease as the residual mode content was suppressed by coiling. To confirm this trend, the MFA values of the PCF and the LCF fibers were calculated from the theoretical MFD values given in Table 1, previously determined for the FM of LP_{01} at a 2-μm light wavelength. Results are represented using a colored line in Fig. 7(d). The good agreement between the measured MFA at D_{SM} and the calculated MFA of the FM confirm that a pure SM regime is reached in both fibers.

It should be noted that, for the SIF under test, multimode operation [illustrated by the measured beam profile Fig. 7(a)] did not allow the evaluation of meaningful MFA values. However, there might be a specific coiling diameter, perhaps between 10 and 60 cm, where a purer SM beam could be achieved due to reduced intermodal coupling.

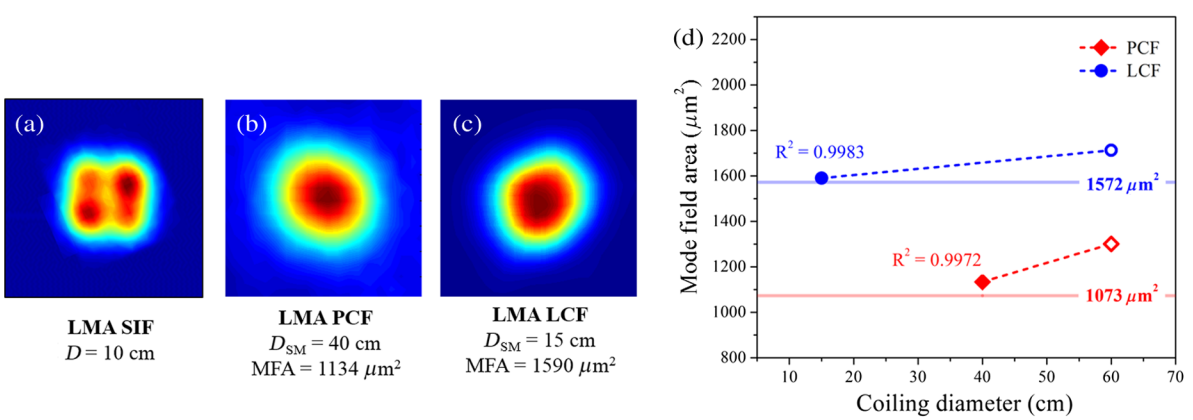

Fig. 7 Measured intensity profiles emerging LMA SIF (a), PCF (b), and LCF (c). (d) Measured mode-field area for different coiling diameters using diamond (PCF) and circle (LCF) shaped markers. Filled symbols indicate SM beams at D_{SM} evaluated from Fig. 6. For comparison, the fundamental mode MFAs (at 2-μm light wavelength) were calculated for each fiber and represented using a matched-colored line.

5 Summary and Conclusion

In summary, S^2 imaging has been performed using a 2-μm light to characterize and compare the performances of three LMA fibers in terms of SM delivery and available MFA. After proving that light guided and propagating in unperturbed LMA fiber designs is, in the case of the PCF and LCF, slightly multimode (with a residual amount of power carried by the first HOM LP_{11}) or in the SIF, clearly multimode, we demonstrated efficient HOM suppression in the PCF and the LCF designs under specific coiling diameters.

From the three samples investigated, we could determine that the PCF and the LCF designs appear to be the most promising candidates to ensure stable, SM, high efficiency, and high quality 2-μm laser emission. These LMA designs outperform the SIF, delivering SM beam purity higher than 98% after coiling PCF and LCF with diameters of 40 and 20 cm, respectively, where the maximum SM purity achieved in the SIF did not exceed 90% under a coiling diameter as small as 10 cm due to residual intermodal coupling. On the other hand, the LCF design, originally not designed for SM operation at 2 μm light wavelength, was measured delivering an ultrapure, low loss SM regime for coiling diameters around 15 cm. This corresponds to more than 99.9% of the light carried by the FM with an available mode-field area of $\sim$1600 μm^2, making this design a serious candidate for further power scaling of fiber lasers.

Results from this study can be used for guidance when developing novel LMA fiber designs for high performance fiber laser applications at 2 μm. It is important to note that other LMA fiber designs have been proposed and have been demonstrated to be suitable for SM, and Tm-doped fiber laser applications, in particular large-pitch fibers with $\sim$60-μm MFD.[10] Most recently, novel Tm-doped PCF designs have been numerically proposed showing the potential to deliver robust SM operation with $\sim$80-μm MFD,[27] indicating a significant ability in finding appropriate LMA fiber designs to sustain power scaling applications and further improve laser performances.

Acknowledgments

This work is supported by HEL-JTO through grants W911NF-10-1-0441 and W911NF-12-1-0450.

References

1. P. Sprangle et al., "Incoherent combining and atmospheric propagation of high-power fiber lasers for directed-energy applications," *IEEE J. Quantum Electron.* **45**(2), 138–148 (2009).
2. G. J. Koch et al., "High energy 2 μm Doppler lidar for wind measurements," *Opt. Eng.* **46**(11), 116201 (2007).
3. J. Cariou, B. Augere, and M. Valla, "Laser source requirements for coherent lidars based on fiber technology," *C. R. Phys.* **7**(2), 213–223 (2006).
4. N. M. Fried, "Thulium fiber laser lithotripsy: an in vitro analysis of stone fragmentation using a modulated 110-watt thulium fiber laser at 1.94 μm," *Laser Surg. Med.* **37**(1), 53–58 (2005).
5. D. Creeden et al., "Mid-infrared ZnGeP2 parametric oscillator directly pumped by a pulsed 2 μm Tm-doped fiber laser," *Opt. Lett.* **33**(4), 315–317 (2008).
6. P. F. Moulton et al., "Tm-doped fiber lasers: fundamentals and power scaling," *IEEE Sel. Top. Quantum Electron.* **15**(1), 85–92 (2009).
7. T. S. McComb et al., "High-power widely tunable fiber lasers," *Appl. Opt.* **49**(32), 6236–6242 (2010).
8. N. Modsching et al., "Lasing in thulium-doped polarizing photonic crystal fiber," *Opt. Lett.* **36**(19), 3873–3875 (2011).
9. C. Gaida et al., "Cw-lasing and amplification in Tm3+-doped photonic crystal fiber rod," *Opt. Lett.* **37**(21), 4513–4515 (2012).
10. F. Jansen et al., "High-power very large mode-area thulium-doped fiber laser," *Opt. Lett.* **37**(21), 4546–4548 (2012).
11. P. Kadwani et al., "Comparison of higher-order mode suppression and Q-switched laser performance in thulium-doped large mode area and photonic crystal fibers," *Opt. Express* **20**(22), 24295–24303 (2012).
12. B. Ward, C. Robin, and I. Dajani, "Origin of thermal modal instabilities in large mode area fiber amplifiers," *Opt. Express* **20**(10), 11407–11422 (2012).
13. H. Otto et al., "Temporal dynamics of mode instabilities in high-power fiber lasers and amplifiers," *Opt. Express* **20**(14), 15710–15722 (2012).
14. A. E. Siegman, "How to (maybe) measure laser beam quality," in *OSA DPSS (Diode Pumped Solid State) Lasers: Applications and Issues*, MQ1, Washington DC (1998).
15. ISO 11146-2, "Test methods for laser beam widths, divergence angles and beam propagation ratios. Part 2: general astigmatic beams," ISO (2005).
16. S. Wielandy, "Implication of higher-order mode content in large mode area fibers with good beam quality," *Opt. Express* **15**(23), 15402–15409 (2007).
17. Y. Tang et al., "High-power narrow-bandwidth fiber laser with an all-fiber cavity," *Opt. Express* **20**(16), 17539–17544 (2012).
18. P. Kadwani et al., "Q-switched thulium-doped photonic crystal fiber laser," *Opt. Lett.* **37**(10), 1664–1666 (2012).
19. L. Dong et al., "Ytterbium-doped all glass leakage channel fibers with highly fluorine-doped silica pump cladding," *Opt. Express* **17**(11), 8962–8969 (2009).
20. C. Jollivet et al., "Low-loss, single-mode propagation in large-mode area leakage channel fiber from 1 to 2 μm," in *CLEO Technical Digest*, CM3I.4, OSA, San Jose (2013).
21. J. W. Nicholson et al., "Spatially and spectrally resolved imaging of modal content in large-mode area fibers," *Opt. Express* **16**(10), 7233–7243 (2008).
22. J. W. Nicholson et al., "Measuring the modal content of large-mode area fibers," *IEEE J. Sel. Topics Quantum Electron.* **15**(1), 61–70 (2009).
23. H. Otto et al., "Improved modal reconstruction for spatially and spectrally resolved imaging," *J. Lightwave Technol.* **31**(8), 1295–1299 (2013).
24. C. Jollivet et al., "Detailed characterization of optical fibers by combining S2 imaging with correlation filter mode analysis," *J. Lightwave Technol.* **32**(6), 1068–1074 (2014).
25. D. Marcuse, "Field deformation and loss caused by curvature of optical fibers," *J. Opt. Soc. Am. B* **66**(4), 311–320 (1976).
26. R. T. Schermer, "Mode scalability in bent optical fibers," *Opt. Express* **15**(24), 15674–15701 (2007).
27. E. Coscelli et al., "Thermally resilient Tm-doped large mode area photonic crystal fiber with symmetry-free cladding," *Opt. Express* **22**(8), 9707–9714 (2014).

Biographies of the authors are not available.